Anomalous magnetotransport in $SrRuO_3$ films: A crossover from Fermi-liquid to non-Fermi-liquid behavior

L. M. Wang
Department of Electrical Engineering, Da-Yeh University, Chang-Hwa 515, Taiwan

H. E. Horng
Department of Physics/Institute of Electro-optical Science and Technology, National Taiwan Normal University, Taipei 116, Taiwan

H. C. Yang*
Department of Physics, National Taiwan University, Taipei, Taiwan
(Received 9 February 2004; revised manuscript received 7 May 2004; published 29 July 2004)

The crystal structures, magnetizations, and magnetotransport properties of $SrRuO_3$ (SRO) films grown on $SrTiO_3$ (STO) substrates are studied. The crystal structures of SRO films show a [110]-oriented and a [010]-oriented epitaxially growth for films deposited on the STO(001) and STO(110) substrates, respectively. The low-temperature magnetization follows the Bloch law both for the $SRO[110]_{oriented}$ and $SRO[010]_{oriented}$ films, while the magnetization near T_C follows the scaling law, $M \propto (T_C - T)^{\alpha}$, with $\alpha = 0.43$ and 0.34 for $SRO[110]_{oriented}$ and $SRO[010]_{oriented}$ films, respectively, indicating the nature of magnetic anisotropy in SRO. Furthermore, a crossover from a T^2 to a $T^{1.5}$ temperature dependence of resistivity corresponding to the Fermi-liquid to non-Fermi-liquid crossover at around 30–40 K has been observed both in the $SRO[110]_{oriented}$ and $SRO[010]_{oriented}$ films. In the paramagnetic regime, the magnetoresistance shows a strong H^2 dependence at the low-field region. These results will be discussed within existing theoretical frames and lead to the conclusion that the fluctuation-induced strongly correlative electrons dominate the non-Fermi-liquid transport properties from the ferromagnetic regime to the paramagnetic regime.

DOI: 10.1103/PhysRevB.70.014433 PACS number(s): 75.40.Cx, 75.47.−m, 75.70.−i, 61.10.Nz

I. INTRODUCTION

Ruthenium oxides, exhibiting a wide range of physical properties such as superconductivity, metallic ferromagnetism, and insulating antiferromagnetism, have been the subject of intense study. One of the ruthenium oxides that has attracted much attention is $SrRuO_3$ (SRO), which shows a variety of interesting electronic and magnetic properties. SRO is a $GdFeO_3$-type distorted perovskite structure,[1] the only example of ferromagnetism in a conducting 4*d* transition-metal oxide, and an intriguing magnetic system with some anomalous features observed. Specific heat measurements,[2] photoemission studies,[3] and low-temperature susceptibility measurements[4] have shown results for density of states and bandwidth that differ from the prediction of band theory. In addition, transport studies of SRO show unusual aspects at high temperatures, where the resistivity increases linearly with temperature, passing through the Ioffe-Regel limit without saturation.[5] This phenomenon has been regarded as suggestive of non-Fermi-liquid behavior, or so-called "bad metal" behavior. The properties of these bad-metal materials with $k_F l \leqslant O(1)$ are not well described within the present theoretical frames, and have focused a great deal of interest during the past years. Some characteristics of SRO still require more experimental information and explanations even though a large number of studies have been done. The first point to note is the Fermi-liquid (FL) to non-Fermi-liquid (NFL) crossover occurring at temperatures around 10–30 K. Kostic *et al.*[6] have found unusual frequency dependences at 40 K in their infrared conductivity measurements. Meanwhile, Mackenzie *et al.*[7] have reported the observation of quantum oscillations in the electrical resistivity of a SRO film, and strongly suggested that the ground state of SRO is a Fermi liquid. A close study on the breakdown of the FL state has been made by Laad and Müller-Hartmann,[8] in which they further confirm the significance of the electronic correlations in SRO. Thus it should be expected that the magnetotransport properties will respond to the FL to NFL crossover. Indeed, some studies[2,9] have observed a small but significant enhancement in $d\rho/dT$ for SRO in the range of 30–40 K. However, no detailed discussions have been given so far for this phenomenon. Similar observations of the crossover from a low-temperature FL regime to a high-temperature bad-metal behavior have been explored in the perovskites of $Ca_{1-x}Sr_xVO_3$ (Ref. 10) and $BaRuO_3$ (Ref. 11) or the itinerant ferromagnetic MnSi (Ref. 12), an interesting subject that merits further investigation.

In this work, we will report on the crystal structures, magnetizations, and magnetotransport properties of SRO films grown on $SrTiO_3$ (STO) substrates. The crystal structures characterized by the x-ray diffraction technique show an epitaxial growth for our SRO films. In the magnetization measurement, the low-temperature Bloch-law behavior and the scaling law $M \propto (T_C - T)^{\alpha}$ near T_C have been observed, showing the nature of magnetic anisotropy in SRO, where M is the magnetization, T is the temperature, and T_C is the Curie temperature. Furthermore, in the transport-property measurements, a crossover from the FL state to the NFL state can be observed at around 30 K, and will be discussed within existing theoretical frames. It is argued that the fluctuation-

induced strongly correlative electrons dominate the NFL transport properties. Finally, we report the H^2 dependence of magnetoresistance (MR) observed in the paramagnetic region and explain it by the spin-disorder scattering process. It is found that the local spin fluctuations further govern the magnetotransport properties from the ferromagnetic regime to the paramagnetic regime.

II. EXPERIMENT

Expitaxial SRO films were grown on STO(001) and STO(110) substrates by the off-axis magnetron sputtering technique. The sputtering gas was a mixture of argon and oxygen gas (3:7). The sputtering pressure was kept at 300 mtorr and the deposition temperature was held at 650 °C. Two films reported here were grown simultaneously during the deposition process. After the deposition, oxygen gas at 1 atm pressure was introduced into the chamber. The cooling rate was 5 °C/min and the films were maintained at growth temperature for 1 h before the cooling process. The as-grown films with a thickness of 100 nm were characterized by an x-ray diffractometer using Cu K_α radiation. For transport measurements, films were photolithographically patterned to a 100-μm long by 50-μm wide bridge. The resistivities and magnetizations of films were measured by the standard four-terminal method, and by a superconducting quantum interference device magnetometer, respectively.

III. RESULTS AND DISCUSSION

A. Crystal structure and magnetic properties of as-grown films

Figures 1(a) and 1(b) show the typical $\theta-2\theta$ x-ray diffraction spectra of SRO films grown on STO(001) and STO(110) substrates, respectively. In Fig. 1(a), only the (110) and (220) peaks of the film are observed, indicating that a highly oriented film is obtained. In Fig. 1(b), only the (020) and (040) peaks of SRO are observed, also indicating that the film reveals a highly oriented growth. The bulk SRO has been regarded as an orthorhombic phase with lattice parameters a =5.570 Å, b=5.530 Å, and c=7.856 Å,[13] while STO has a cubic perovskite structure with a lattice constant of 3.905 Å. According to the peak positions shown in Fig. 1(a), the SRO film grown onto STO(001) substrate is [110] oriented normal to the substrate with an out-of-plane lattice parameter of d_{110}=3.949 Å, which is close to that of 3.96 Å obtained by Gan *et al.*,[14] and is slightly greater than the bulk value of $\sqrt{a^2+b^2}/2$=3.924 Å. On the other hand, according to Fig. 1(b), the SRO film grown on STO(110) has the [010] orientation normal to the substrate with an out-of-plane lattice parameter of d_{010}=5.527 Å, which is very close to the bulk value. The small deviation of the lattice parameter from the bulk value implies a smaller strain effect in the SRO film grown on STO(110) substrate. The insets of Figs. 1(a) and 1(b) show the crystal-growth orientation relationship between the SRO films and substrates of STO(001) and STO(110), respectively. Generally, SRO films are grown with out-of-plane directions of SRO[110]∥STO[001] and SRO[010]∥STO[110] for used substrates of STO(001) and STO(110), respectively. Thereafter, we denominate the former $\mathrm{SRO[110]_{oriented}}$ and the latter $\mathrm{SRO[010]_{oriented}}$, respectively. It has been pointed out that the $\mathrm{SRO[110]_{oriented}}$ film is possibly grown with the coexistence of the in-plane orientation relationship of SRO[$\bar{1}$10]∥STO[100], SRO[001]∥STO[010], and SRO[$\bar{1}$10]∥STO[010], SRO[001]∥STO[100],[14] which is indistinguishable in our x-ray in-plane scans. Otherwise, the in-plane orientation for $\mathrm{SRO[010]_{oriented}}$ film is found to have the crystal structure relationships of SRO[001]∥STO[001] and SRO[100]∥STO[1$\bar{1}$0], which coincides with the lattice parameters of $d_{\mathrm{SRO[001]}}$=7.86 Å≈2$d_{\mathrm{STO[001]}}$, and $d_{\mathrm{SRO[100]}}$ =5.57 Å≈2$d_{\mathrm{STO[1\bar{1}0]}}$, respectively. The x-ray ϕ scans for our $\mathrm{SRO[110]_{oriented}}$ and $\mathrm{SRO[010]_{oriented}}$ films will be presented and discussed elsewhere.

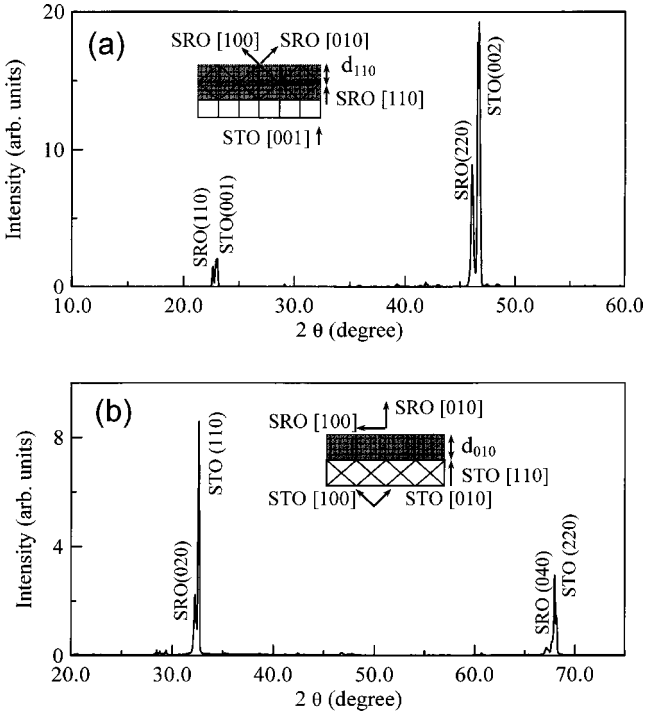

FIG. 1. X-ray diffraction patterns of SRO films grown on (a) STO(001) and (b) STO(110) substrates. The inset shows the relationship of crystal-growth orientation.

Figures 2(a) and 2(b) show the temperature dependence of magnetization for $\mathrm{SRO[110]_{oriented}}$ and $\mathrm{SRO[010]_{oriented}}$ films, respectively, with an applied field of 100 G perpendicular to the substrate plane. The spontaneous magnetization near T_C follows the scaling law $M \propto (T_C - T)^\alpha$ with α =0.43, T_C=137 K, and α=0.34, T_C=160 K for $\mathrm{SRO[110]_{oriented}}$ and $\mathrm{SRO[010]_{oriented}}$ films, respectively. The value of exponent α remains controversial. Klein and co-workers[5,15] obtained the exponent α=0.325 and interpreted it with an Ising behavior, while Kim *et al.*[16] found α=0.5 and regarded it as a mean-field behavior. The obvious difference in α between our $\mathrm{SRO[110]_{oriented}}$ and $\mathrm{SRO[010]_{oriented}}$ films implies that the critical exponent seems to be dependent on the magnetization orientation. This

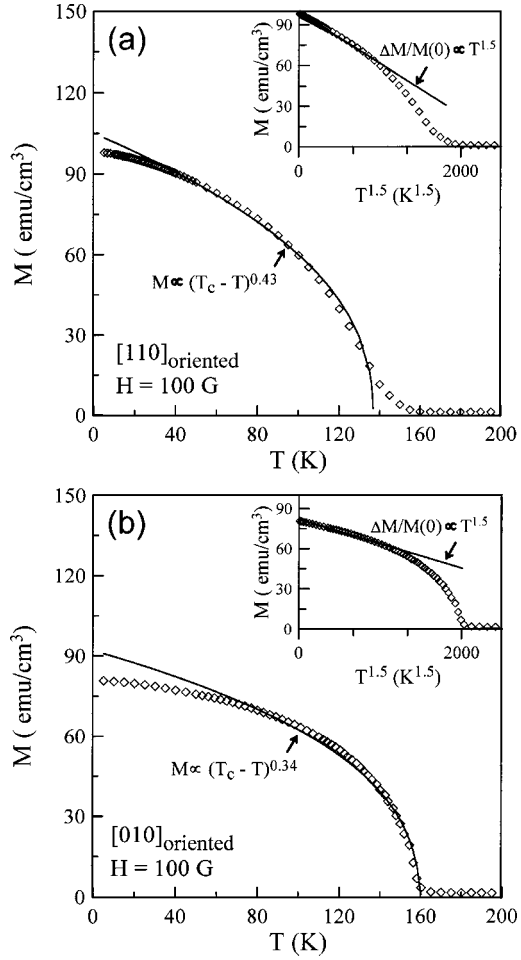

FIG. 2. Magnetizations of (a) $SRO[110]_{oriented}$ and (b) $SRO[010]_{oriented}$ films in $H=100$ G. The solid lines are the fitted curves by $M \propto (T_C - T)^{\alpha}$. The insets show $T^{1.5}$ plots of magnetization for the corresponding sample and the straight lines are the Bloch-law fitting.

is in accordance with the nature of magnetic anisotropy in SRO as reported.[4] In addition, the suppression of T_C observed in the $SRO[110]_{oriented}$ film may be due to the larger strain that changes the Ru-O-Ru interatomic distance or bonding angles, consequently reducing the exchange energy among spins, and is responsible for the suppression of the Curie temperature. The insets of Figs. 2(a) and 2(b) show the $T^{1.5}$ plots of magnetization for $SRO[110]_{oriented}$ and $SRO[010]_{oriented}$ films, respectively. According to the Bloch-law theory, in the low-temperature limit, the dominant excitations known to suppress magnetization are spin-wave excitations, which suppress the magnetization as $\Delta M(T)/M(0) = \lambda T^{1.5}$. In this model $\lambda = (0.0587/S)(k_B/2JS)^{1.5}$ for the simple pseudocubic magnetic lattice of Ru^+, where S is the total spin of Ru^+, and J is the exchange interaction between two neighboring Ru^+ ions. Taking $S=1$, we obtain $J=14.41$ and 20.57 k_BK for $SRO[110]_{oriented}$ and $SRO[010]_{oriented}$ films, respectively, which is comparable to that of 26.33 k_BK reported.[17] The larger exchange energy for $SRO[010]_{oriented}$ films is in agreement with the higher T_C observed.

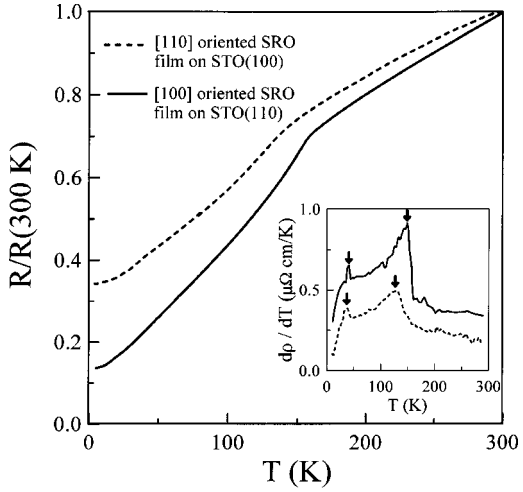

FIG. 3. Temperature dependence of the normalized resistance $R/R(300\ \mathrm{K})$ for $SRO[110]_{oriented}$ and $SRO[010]_{oriented}$ films at zero field. The inset is the temperature dependence of the resistivity derivative $d\rho/dT$. Arrows indicate the jump in $d\rho/dT$.

B. Transport properties of as-grown films

The transport properties are expected to be influenced by the crystal structure and anisotropic magnetization. Figure 3 shows the temperature dependence of the normalized resistance $R/R(300\ \mathrm{K})$ for $SRO[110]_{oriented}$ and $SRO[010]_{oriented}$ films at zero field. The resistance-temperature curves exhibit a pronounced bend at around Curie temperature. Also shown in the inset of Fig. 3 is the temperature dependence of the resistivity derivative, $d\rho/dT$. At T_C, the resistivity has a break in slope and therefore $d\rho/dT$ jumps as reported by previous workers.[2,9,15,16] Kim *et al.*[16] have recently demonstrated the Fisher-Langer relation and the existence of fluctuation near T_C, according to the overlap between their background-subtracted specific heat and $d\rho/dT$. However, it is interesting that another pronounced $d\rho/dT$ jump at around 30–40 K can be observed both in our $SRO[110]_{oriented}$ and $SRO[010]_{oriented}$ films, implying an occurrence of phase transition within the temperature region. This low-temperature anomaly has not been particularly discussed yet. In Ref. 2, Allen *et al.* observed the enhancement in $d\rho/dT$ in the range of 35–45 K, where their specific-heat measurement (without background subtracted) did not show any significant anomaly, and argued that this effect is sample-dependent. Actually, in an early study, Kanbayasi[18] has found a dramatic change in magnetocrystalline anisotropy in this low-temperature region, where the $d\rho/dT$ is expected to be affected not only by $\langle M \rangle$, but also by $\langle \Delta M^2 \rangle$.[16] The observation of no significant specific-heat anomaly in the low-temperature region may be due to the extremely small variation in specific heat, and a precisely subtracted background needs to be taken into account. It merits further consideration with more experimental work. The low-temperature anomaly in $d\rho/dT$ in our observation not only implies the change in ρ-T behavior, but also corresponds to the FL-NFL crossover observed in the quantum-oscillation study at extremely low temperatures[7] and the unusual infrared-conductivity behavior for $T > 40$ K. In the following discussion, the magnetotrans-

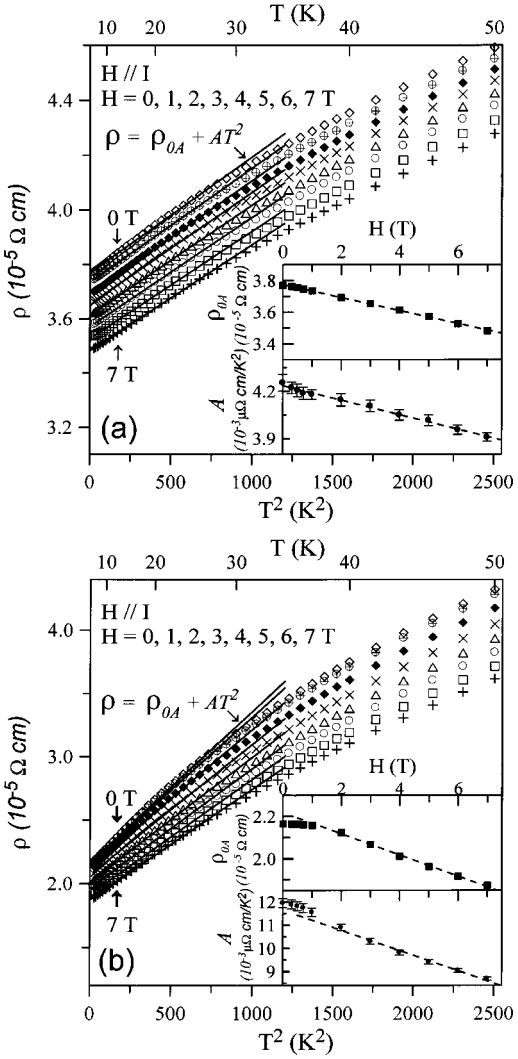

FIG. 4. Low-temperature resistivities of (a) SRO[110]$_{\text{oriented}}$ and (b) SRO[010]$_{\text{oriented}}$ films in a magnetic field as a function of T^2. The solid lines are the fitting of $\rho=\rho_{0A}+AT^2$. The insets show the field dependences of ρ_{0A} and A for corresponding data and the straight dashed lines correspond to a linearly field dependence.

port properties of SRO with their mechanisms will be explored.

Figures 4(a) and 4(b) show that the resistivities of the as-grown films follow approximately the form $\rho=\rho_{0A}+AT^2$ at temperatures below 25 K with applied fields parallel to the current I. Here the resistivities in different fields are affected by the spin-flip scattering, without the Lorentz contribution due to $H\|I$. As shown in Figs. 4(a) and 4(b), the residual resistivity ρ_{0A} and the value of A are field-dependent, and reveal negative MR, the characteristics of ferromagnetic compounds. The insets of Figs. 4(a) and 4(b) show the field dependences of ρ_{0A} and A for SRO[110]$_{\text{oriented}}$ and SRO[010]$_{\text{oriented}}$ films, respectively. In zero field, the residual resistivities $\rho_{0A}=3.8\times10^{-5}$ and $2.2\times10^{-5}\ \Omega$ cm, respectively, for our SRO[110]$_{\text{oriented}}$ and SRO[010]$_{\text{oriented}}$ films are close to that reported for single-crystal samples.[2] Moreover, as shown in the insets of Figs. 4(a) and 4(b), a linear dependence of ρ_{0A} vs H at high-field region can be observed both in the SRO[110]$_{\text{oriented}}$ and SRO[010]$_{\text{oriented}}$ films. Furthermore, the values of A are found to be 4.2×10^{-3} and $1.2\times10^{-2}\ \mu\Omega$ cm/K^2 at $H=0$ for the SRO[110]$_{\text{oriented}}$ and SRO[010]$_{\text{oriented}}$ films, respectively, which are comparable to that of $2.5\times10^{-3}\ \mu\Omega$ cm/K^2 for $BaRuO_3$ (Ref. 11) and $3.4\times10^{-2}\ \mu\Omega$ cm/K^2 for metallic perovskite $LaNiO_3$ (Ref. 19). Within the standard free-electron model, an empirical relationship has been found between coefficient A and the coefficient γ of the electronic specific heat by Kadowaki and Woods:[20] $A/\gamma^2=1\times10^{-5}\ \mu\Omega$ cm/(mole K/mJ)^2. Using our experimental values of A and $\gamma=30$ mJ/mole K^2,[2,4] we have $A/\gamma^2=0.5\times10^{-5}$ and $1.3\times10^{-5}\ \mu\Omega$ cm/(mole K/mJ)^2 for our SRO[110]$_{\text{oriented}}$ and SRO[010]$_{\text{oriented}}$ films, respectively, which agree with the Kadowaki-Woods ratio.

It is noticed that the contribution of electron-magnon scattering also provides a T^2 temperature dependence of resistivity. Mannari[21] has demonstrated that the electron-magnon resistivity should be expressed by

$$\rho_{electron\text{-}magnon}=A_{e\text{-}m}T^2=\frac{3\pi^5}{16}\frac{S}{e^2}\left(\frac{\mu}{m_e}\right)^2\frac{k_B^2N^2J^2(0)}{E_F^4}\frac{h}{2\pi k_F}T^2, \tag{1}$$

where μ is the effective mass of magnon, $NJ(0)$ is the spin-orbit coupling energy, E_F is the Fermi energy, and k_F is the wave vector at the Fermi surface. Mannari obtained $A_{e\text{-}m}=1.1\times10^{-5}\ \mu\Omega$ cm/K^2 for the Ni metal. For SRO, taking $E_F=1.4$ eV for $T<T_C$,[22] the Fermi velocity $V_F=1\times10^5$ m/s,[2] and $NJ(0)=0.4$ eV,[8] into Eq. (1), we obtain $A_{e\text{-}m}\approx4.15\times10^{-4}\ \mu\Omega$ cm/K^2 for SRO, which is more than one order of magnitude larger than that for Ni, but is about several percent of the ratio compared with our experimental values. However, the strong field dependence of coefficient A as seen in the insets of Figs. 4(a) and 4(b) cannot be well explained by taking account of electron-electron scattering only because a weak field dependence of A is expected in the FL regime. In the presence of a magnetic field, the coupling between electrons and magnons will produce significant spin-flip scattering, and therefore coefficient A is expected to be dependent on the field. From this, we see that the electron-magnon scattering considered here has a small but non-negligible contribution to resistivity. The field dependence of resistivity coefficient A has also been observed on the doping manganite $La_{0.67}(Pb,Ca)_{0.33}MnO_3$ single crystals by Jaime *et al.*[23] They attributed the T^2 temperature dependence of resistivity to a single-magnon scattering and extended Mannari's calculation to support their ideas. According to their calculation, the effect of an applied field is to open a gap $\Delta=g\mu_BH$ in the magnon spectrum with the result that $A(0)-A(H)\propto\Delta\propto H$. This field dependence of coefficient A is similar in behavior to that observed in our SRO films. Thus, the linear field dependence of resistivity coefficient A may be attributed to the effect of electron-magnon scattering.

Figures 5(a) and 5(b) illustrate the $T^{1.5}$ temperature dependence of resistivity for SRO[110]$_{\text{oriented}}$ and SRO[010]$_{\text{oriented}}$ films, respectively. It can be seen that the resistivity can be described by $\rho=\rho_{0B}+BT^{1.5}$ over a wide temperature range of $\sim$50–120 K. The top insets of Figs. 5(a) and 5(b) show the

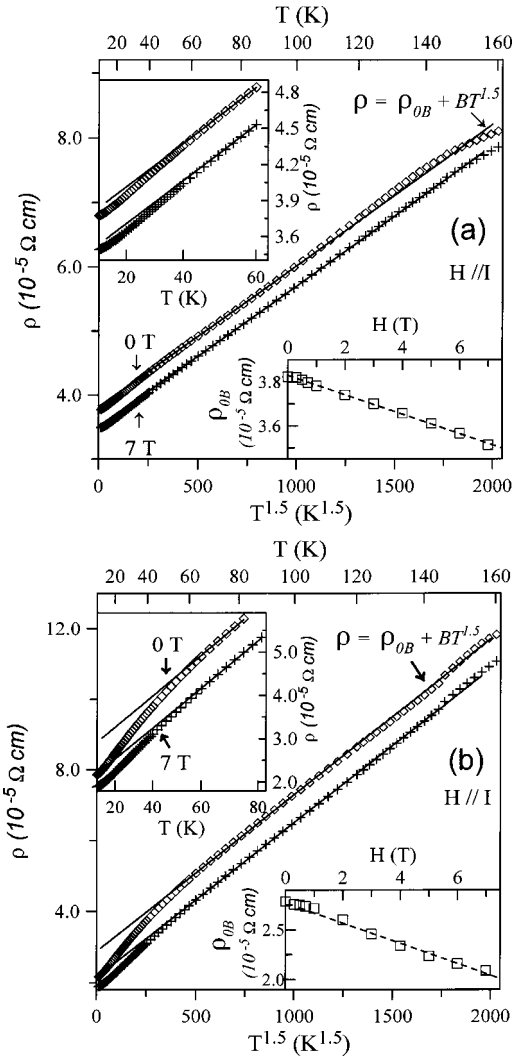

FIG. 5. Resistivities of (a) $SRO[110]_{oriented}$ and (b) $SRO[010]_{oriented}$ films in $H=0$ and 7 T vs $T^{1.5}$. The solid lines are the fitting of $\rho=\rho_{0B}+BT^{1.5}$. The top insets show the resistivity crossover from T^2 to $T^{1.5}$ dependence at around 40 K. The insets show the field dependence of ρ_{0B} for corresponding data and the straight dashed lines correspond to a linear dependence.

resistivity crossover from a T^2 to a $T^{1.5}$ dependence at around 40 K, which is near the second $d\rho/dT$-enhancement temperature as shown in the inset of Fig. 3. It is worth noting that coefficient B is almost independent of the applied field, while the residual resistivity ρ_{0B} decreases linearly with an increase in applied field for both $SRO[110]_{oriented}$ and $SRO[010]_{oriented}$ films as seen in the lower insets of Figs. 5(a) and 5(b), respectively. The origin of the NFL behavior for SRO has been investigated by Laad and Müllier-Hartmann.[8] They provided a model to explain the NFL features observed in the optical response of SRO for $T>40$ K, in which a NFL metallic state can be affected by the t_{2g} orbital orientation in an almost cubic structure. However, in this temperature regime the transport behaviors have not been debated yet. Here this unusual $T^{1.5}$ law observed in the transport properties of the SRO films will be discussed below.

A contribution to the resistivity from the incoherent part of electron-magnon scattering has been found to be proportional to $T^{1.5}$ by Mills *et al.*[24] However, Mazin and Singh[25] have estimated the characteristic magnon energy k_BT_m for SRO and obtained $T_m\approx 70$ K. Thus, we infer that the $T^{1.5}$ law observed in the wide temperature range of 50–120 K cannot be interpreted only with the electron-magnon scattering. A recent study done by Rivadulla *et al.*[26] showed that the unconventional $T^{1.5}$ temperature dependence of the resistivity can also be observed in several strongly correlated systems such as $Na_{0.5}CoO_2$ or $CaVO_3$. They proposed a model in which the scattering of the conduction electrons by locally cooperative bond-length fluctuations and FL electrons are taken into account to describe this behavior. Some other mechanisms, such as self-consistent renormalization theory,[27] that can also produce the $T^{1.5}$ law of resistivity have been discussed by Rivadulla *et al.* and have been excluded in their case because no evidence of antiferromagnetic fluctuation can be found in the metallic phase. This consideration is applicable to the SRO which shows ferromagnetic fluctuation only. Furthermore, we obtain the values of coefficient $B=2.2\times10^{-8}$ and 4.4×10^{-8} Ω cm $K^{-1.5}$ for our $SRO[110]_{oriented}$ and $SRO[010]_{oriented}$ films, respectively, which are close to that of $\sim3\times10^{-8}$ Ω cm $K^{-1.5}$ for $Na_{0.5}CoO_2$ and $\sim5\times10^{-8}$ Ω cm $K^{-1.5}$ for $CaVO_3$ estimated from the data of Rivadulla *et al.* Thus, we infer that the mechanism of scattering between fluctuation-induced localized electrons and FL electrons is applicable to SRO for describing the $T^{1.5}$ temperature dependence of resistivity. Additionally, it is noteworthy that an earlier theoretical work[28] also proposed a similar NFL behavior of $\rho\propto T^{1.56}$ within the framework of a self-consistent spin fluctuation theory for three-dimension ferromagnetism. Although the mechanism of resistivity in this theory seems to be different from that proposed by Rivadulla *et al.*, both theories give the consistent picture that spin fluctuations play an important role for NFL behavior in SRO.

Figures 6(a) and 6(b) show the temperature dependence of the longitudinal MR ratio, defined by $MR=[\rho(H)-\rho(0)]/\rho(0)$, in fields of $H=2$, 4, and 6 T along the direction of applied current. We can see that the MR is negative, reaching a local minimum at around T_C, and shows a second local minimum at temperatures around 25 K, near the FL-NFL crossover temperature. On the other hand, in the paramagnetic regime the magnitude of MR monotonically decreases with an increase in temperature. An interesting issue is whether the MR behavior is affected by the spin fluctuation at temperatures above T_C, and therefore it is important to examine how the change in resistivity correlates with magnetic ordering. Shown in the inset of Fig. 6 is the MR as a function of the square of normalized magnetization M/M_{max} for $SRO[110]_{oriented}$ and $SRO[010]_{oriented}$ films with an applied field of 2 T. The MR-$(M/M_{max})^2$ curves were obtained using the MR(T) and M(T) data, where M_{max} was taken by $M_{max}=M(5\text{ K}, H=2\text{ T})$, the magnetization at the lowest temperature in our measurement.

For several ferromagnetic pervovskite oxides,[29,30] it has been reported that in the low-M regime, the electrical resistivity and magnetization can be approximately described by

$$\mathrm{MR}=[\rho(H)-\rho(0)]/\rho(0)=-C[M(H)/M_{max}]^2. \quad (2)$$

This origin of $\mathrm{MR}\propto M^2$ can be explained by the carrier scattering due to the thermally fluctuating spins, or the spin-

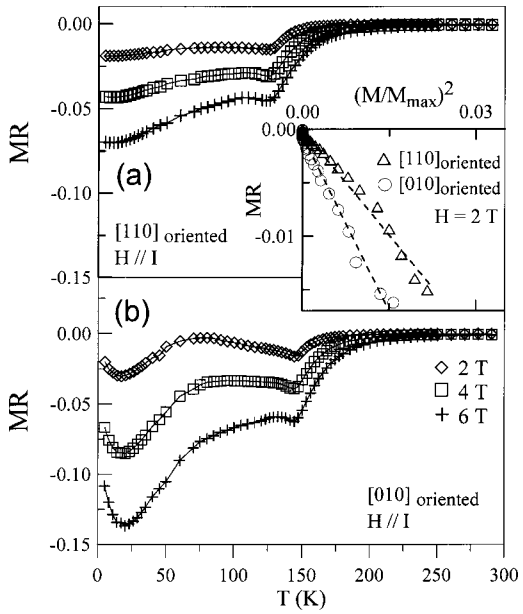

FIG. 6. Longitudinal MR as a function of temperature in fields of $H=2$, 4, and 6 T for (a) SRO$[110]_{\text{oriented}}$ and (b) SRO$[010]_{\text{oriented}}$ films. The inset is the MR as a function of the square of normalized magnetization $M/M_{\max}$ and the dashed lines are the fitted lines by Eq. (2).

disorder scattering. When the induced magnetic moment is developed, the amplitude of the spin fluctuation decreases so that the resistivity $\rho(H)$ decreases, and therefore the magnitude of MR increases. Furukawa[31] has calculated coefficient C in terms of the Kondo lattice model with ferromagnetic exchange interaction and showed that it is related to the coupling between moving carriers and the localized spins, i.e., the Hund coupling. The calculated value of C is about $4-5$ in the case of strong coupling, but becomes $C\approx 1$ in the weak coupling limit. As seen in the inset of Fig. 6, the MR follows the expression of Eq. (2) for both SRO$[110]_{\text{oriented}}$ and SRO$[010]_{\text{oriented}}$ films. We obtain $C\approx 0.7$ and 1.1 for the SRO$[110]_{\text{oriented}}$ and SRO$[010]_{\text{oriented}}$ films, respectively. The obtained values of coefficient C imply that the SRO is close to the weak coupling limit, being in correspondence with the weaker Hund coupling of ~ 0.5 eV for SRO (Ref. 6) than that of $\geqslant 4$ eV for the doped $La_{1-x}Sr_xMnO_3$ with $x=0.175$.[32] Otherwise, the obtained smaller value of coefficient C for the SRO$[110]_{\text{oriented}}$ film should be attributable to the effect of structural tuning, which has been observed in the ferromagnetic manganites.[29]

According to Eq. (2), and taking $M=\chi H$ into account, we can easily obtain that the H^2 dependence of MR, MR $=-\beta H^2$, holds with coefficient β being proportional to $1/(T-T_C)^2$ because the susceptibility $\chi(T)$ of this system far above T_C follows a Curie-Weiss paramagnetism: $\chi(T) \propto 1/(T-T_C)$. Figures 7(a) and 7(b) show $-$MR vs H^2 for the SRO$[110]_{\text{oriented}}$ and SRO$[010]_{\text{oriented}}$ films in the paramagnetic regime, respectively. Clearly, a strong H^2 dependence of negative MR is observed both for the SRO$[110]_{\text{oriented}}$ and SRO$[010]_{\text{oriented}}$ films at temperatures above 180 K. Below 180 K, the H^2 dependence of $-$MR holds only in the low-field region. The deviation from H^2 behavior for MR in high fields should be due to the nonlinear field dependence of M in the high-field region when the temperature is near T_C. Also shown in the insets of Figs. 7(a) and 7(b) are the β vs T and β^{-1} vs $(T-T_C)^2$ plots. It can be seen that a straight dashed line fits well the data, which is in accord with our deduction. This indicates that magnetotransport originates from the local spin fluctuations. Our results also coincide with the observation of the MR scaling of $H^2/(T-T_C)^2$ for SRO films grown on $LaAlO_3$.[33]

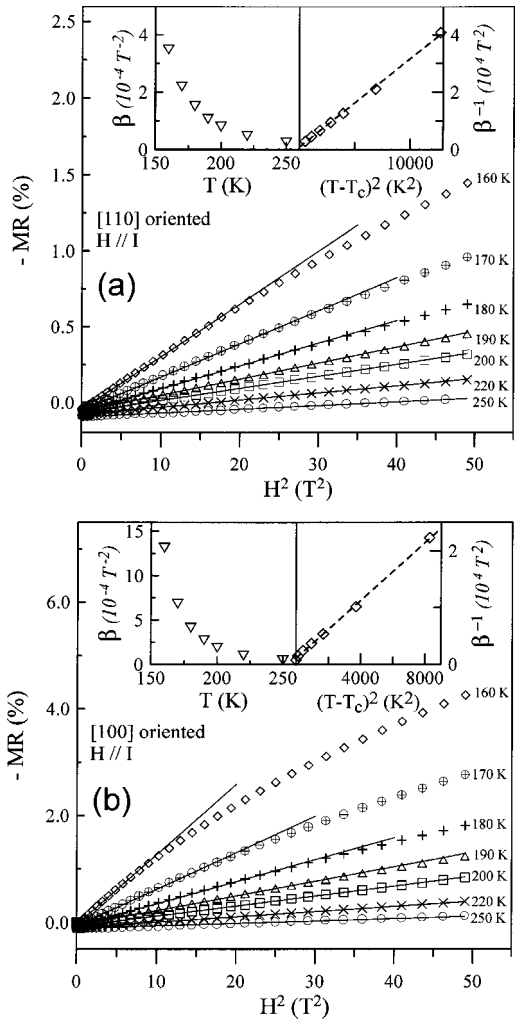

FIG. 7. Negative MR as a function of H^2 for (a) SRO$[110]_{\text{oriented}}$ and (b) SRO$[010]_{\text{oriented}}$ films. The straight lines correspond to a linear fit: $-\text{MR}=\beta H^2$. The insets show the temperature dependence of β and the β^{-1} versus $(T-T_C)^2$ plots.

IV. SUMMARY

In summary, we have reported the crystal structure, magnetization, and magnetotransport properties of SRO films in the ferromagnetic and paramagnetic regimes. The crystal structures of SRO films are characterized by the x-ray diffraction technique and show a [110]-oriented and a [010]-oriented epitaxially growth for films deposited on the STO(001) and STO(110) substrates, respectively. The low-

temperature magnetization follows the Bloch law for both the $SRO[110]_{oriented}$ and $SRO[010]_{oriented}$ films, and a larger exchange integral is obtained in the $SRO[010]_{oriented}$ film, corresponding to a higher T_C observed. In addition, the magnetization near T_C follows the scaling law $M \propto (T_C - T)^{\alpha}$, with $\alpha = 0.43$ and 0.34 for $SRO[110]_{oriented}$ and $SRO[010]_{oriented}$ films, respectively, indicating the nature of magnetic anisotropy in SRO. The crystal structure and anisotropic magnetization are expected to affect the transport properties.

Furthermore, the magnetotransport measurements show a crossover from a T^2 to $T^{1.5}$ temperature dependence of resistivity for both the $SRO[110]_{oriented}$ and $SRO[010]_{oriented}$ films in the ferromagnetic region, which corresponds to the FL-NFL crossover at around 30–40 K, observed in other measurements. The T^2 temperature dependence of resistivity is governed by electron-electron scattering, while the $T^{1.5}$ behavior should be attributed to the scattering of the FL electrons and the localized electrons due to the bond-length fluctuation. On the other hand, in the paramagnetic regime, the MR shows a strong H^2 dependence, and can be explained by the carrier scattering due to the fluctuation spins. The local spin fluctuations further govern the NFL magnetotransport properties from the ferromagnetic regime to the paramagnetic regime.

ACKNOWLEDGMENT

The authors thank the National Science Council of the Republic of China for financial support under Grant Nos. NSC 92-2112-M-212-001 and NSC 92-2112-M002-006. This work was also partially supported by the Da-Yeh University under Grant No. ORD-9303 and by the Ministry of Education under the program of promoting university academic excellence.

*Corresponding author. Email address: hcyang@phys.ntu.edu.tw

[1] T. C. Gibb, R. Greatrex, N. N. Greenwood, and P. Kaspi, J. Chem. Soc. Dalton Trans. **1973**, 1253 (1973).
[2] P. B. Allen, H. Berger, O. Chauvet, L. Forro, T. Jarlborg, A. Junod, B. Revaz, and G. Santi, Phys. Rev. B **53**, 4393 (1996).
[3] K. Fujioka, J. Okamoto, T. Mizokawa, A. Fujimori, I. Hase, M. Abbate, H. J. Lin, C. T. Chen, Y. Takeda, and M. Takano, Phys. Rev. B **56**, 6380 (1997).
[4] G. Cao, S. McCall, M. Shepard, and J. E. Crow, and R. P. Guertin, Phys. Rev. B **56**, 321 (1997).
[5] L. Klein, J. S. Dodge, C. H. Ahn, J. W. Reiner, L. Mieville, T. H. Geballe, M. R. Beasley, and Kapitulnik, J. Phys.: Condens. Matter **8**, 10111 (1996).
[6] P. Kostic, Y. Okada, N. C. Collins, Z. Schlesinger, J. W. Reiner, L. Klein, A. Kapitulnik, T. H. Geballe, and M. R. Beasley, Phys. Rev. Lett. **81**, 2498 (1998).
[7] A. P. Mackenzie, J. W. Reiner, A. W. Tyler, L. M. Galvin, S. R. Julian, M. R. Beasley, T. H. Geballe, and A. Kapitulnik, Phys. Rev. B **58**, R13318 (1998).
[8] M. S. Laad and E. Müller-Hartmann, Phys. Rev. Lett. **87**, 246402 (2001).
[9] M. Izumi, K. Nakazawa, Y. Bando, Y. Yoneda, and H. Teracohi, J. Phys. Soc. Jpn. **66**, 3893 (1997).
[10] I. H. Inoue, I. Hase, Y. Aiura, A. Fujimori, Y. Haruyama, T. Maruyama, and Y. Nishihara, Phys. Rev. Lett. **74**, 2539 (1995).
[11] J. T. Rijssenbeek, R. Jin, Yu. Zadorozhny, Y. Liu, B. Batlogg, and R. J. Cava, Phys. Rev. B **59**, 4561 (1999).
[12] C. Pfleiderer, G. J. McMullan, S. R. Julian, and G. G. Lonzarich, Phys. Rev. B **55**, 8330 (1997).
[13] C. W. Jones, P. D. Battle, P. Lightfoot, and W. T. A. Harrison, Acta Crystallogr., Sect. C: Cryst. Struct. Commun. **45**, 365 (1989).
[14] Q. Gan, R. A. Rao, and C. B. Eom, Appl. Phys. Lett. **70**, 1962 (1997).
[15] L. Klein, J. S. Dodge, C. H. Ahn, G. J. Snyder, T. H. Geballe, M. R. Beasley, and A. Kapitulnik, Phys. Rev. Lett. **77**, 2774 (1996).
[16] D. Kim, B. L. Zink, F. Hellman, S. McCall, G. Cao, and J. E. Crow, Phys. Rev. B **67**, 100406 (2003).
[17] L. Klein, J. S. Dodge, T. H. Geballe, A. Kapitulnik, A. F. Marshall, L. Antognazza, and K. Char, Appl. Phys. Lett. **66**, 2427 (1995).
[18] A. Kanbayasi, J. Phys. Soc. Jpn. **41**, 1879 (1976).
[19] K. Sreedhar, J. M. Honig, M. Darwin, M. McElfresh, P. M. Shand, J. Xu, B. C. Crooker, and J. Spalek, Phys. Rev. B **46**, 6382 (1992).
[20] K. Kadowaki and S. B. Woods, Solid State Commun. **58**, 507 (1986).
[21] I. Mannari, Prog. Theor. Phys. **22**, 335 (1959).
[22] M. Shikano, T-K. Huang, Y. Inaguma, M. Itoh, and T. Nakamura, Solid State Commun. **90**, 115 (1994).
[23] M. Jaime, P. Lin, M. B. Salamon, and P. D. Han, Phys. Rev. B **58**, R5901 (1998).
[24] D. L. Mills, A. Fert, and I. A. Campbell, Phys. Rev. B **4**, 196 (1971).
[25] I. I. Mazin and D. J. Singh, Phys. Rev. B **56**, 2556 (1997).
[26] F. Rivadulla, J.-S. Zhou, and J. B. Goodenough, Phys. Rev. B **67**, 165110 (2003).
[27] Moriya, *Spin Fluctuations in Itinerant Electron Systems* (Springer, Berlin, 1985).
[28] Suresh G. Mishra and P. A. Sreeram, Phys. Rev. B **57**, 2188 (1998).
[29] J. Fontcuberta, B. Martínez, A. Seffar, S. Piñol, J. L. García-Muñoz, and X. Obradors, Phys. Rev. Lett. **76**, 1122 (1996).
[30] S. Yamaguchi, H. Taniguchi, H. Takagi, T. Arima, and Y. Tokura, J. Phys. Soc. Jpn. **64**, 1885 (1995).
[31] N. Furukawa, J. Phys. Soc. Jpn. **63**, 3214 (1994).
[32] N. Furukawa, J. Phys. Soc. Jpn. **64**, 2734 (1995).
[33] J. H. Cho, Q. X. Jia, X. D. Wu, S. R. Foltyn, and M. P. Maley, Phys. Rev. B **54**, 37 (1996).